Penerbit Akademia Baru

Journal of Advanced Research in Applied Sciences and Engineering Technology

Journal homepage: www.akademiabaru.com/araset.html
ISSN: 2462-1943

Effect of Fiber Misalignment on Tensile Response of Unidirectional CFRP Composite Lamina

Open Access

Azisyahirah Azizan[1,*], Haris Ahmad Israr[1], Mohd Nasir Tamin[1]

[1] Center for Composites, Faculty of Mechanical Engineering, Universiti Teknologi Malaysia, 81310 Skudai, Johor Bahru, Malaysia

ARTICLE INFO

Article history:
Received 9 February 2018
Received in revised form 15 March 2018
Accepted 31 March 2018
Available online 1 April 2018

ABSTRACT

Mechanical responses and failure of fiber-reinforced polymer (FRP) composite laminates could be predicted using the validated finite element (FE) simulation. The material constitutive and damage models employed in the simulation are developed based on the properties of the unidirectional lamina, including those obtained through tension tests. Such computational model assumes perfectly aligned fibers in the lamina. In this respect, this paper examined the effect of fabrication-inherited fiber misalignment on the tensile response of the unidirectional lamina. For this purpose, a series of tension tests are performed on unidirectional carbon fiber-reinforced polymer (CFRP) composite lamina specimens with different gage lengths ranging from 50 to 150 mm. Fiber misalignment is quantified to be 7o and represents the nominal deviation of the fibers from the reference longitudinal axis direction. Load-displacement responses of the specimens are compared. Results show that the nominal tensile strength of the lamina is 1089±33 MPa. The elastic modulus, however, increases from 36.96 to 55.93 GPa as the gage lengths vary from 50 to 150 mm, respectively. This is due to the induced bending effects on the reinforcing fibers that is greater for longer gage lengths. Multiple fiber fracture events, each is depicted in a noticeable load drop, are recorded throughout the tensile loading of long lamina specimens. Although the load at fracture is accurately reproduced by the FE simulation using the damage-based mesoscale model, the effect of fiber misalignment could not be captured.

Keywords:
Carbon fiber, fiber misalignment, tensile test

1. Introduction

Among the most fundamental properties of CFRP composite are those obtained from tensile testing of a unidirectional (UD) composite in the fiber direction [1-3]. These properties include modulus of elasticity, Poisson's ratio, tensile strength, and ultimate tensile strain. The tensile test that measures these properties is, on the face of it, very simple: A thin strip of a UD composite is placed into the wedge grips of a mechanical testing machine and loaded slowly in tension. Loading continues to ultimate failure, the point at which tensile strength and ultimate tensile strain are

* *Corresponding author.*
E-mail address: A. Azizan (azisyahirah@gmail.com)

determined [4]. In practice, however, obtaining the desired results can be slightly challenging. Typically, the material properties used for CFRP are those provided by manufacturers and are based on tensile tests of "perfect" coupons [2]. So far, very little attention has been paid to investigate the effect of misalignment of the fiber in the lamina itself. On the other hand, there are concerns about the performance of a component when errors may be resulted from fiber misalignment which has been studied in the literature [6-8]. Such misalignment can occur due to manufacturing deficiency and defects, curved surfaces, and fiber waviness [9]. Depending on the severity of the fiber misalignment, the difference between actual strength and stiffness of the CFRP from the assumed nominal values may become unacceptable or, at least, warrant a reduction of performance expectations.

An experimental investigation on the significant effect of fiber misalignment on stiffness degradation is an essential for the effective use of CFRP component. In this study, a series of tension tests are performed on UD CFRP composite lamina with various gage lengths. The Scanning Electron Microscope (SEM) is utilized in order to quantify the fiber misalignment. As the results, the load-displacement responses are investigated. The results of such an investigation should be implemented into corresponding construction and design specifications for guidance in field practice. Therefore the purpose of this study is to quantify the effect of fiber misalignment in establishing the property of unidirectional fiber-reinforced lamina.

2. Materials and Experimental Procedures

The CFRP composite lamina is made up using unidirectional pre-impregnated high modulus carbon fibers and epoxy resin. The cured lamina with thickness 0.22mm was cut into specimens in several different length as described in Table 1.

Figure 1 illustrates the specimen dimension with reference 0°fiber orientation along the length of the specimen. Note that the gage length suggested by ASTM D3039 [5] is 138mm. 40mmm x 15mm Aluminium tapered tab which is bonded to the lamina using Araldite adhesive is used in order to increase the area the loading region and, thus, reducing the local stress concentration. In addition, it is used to protect the specimen from damage by the grips that clamp the specimen ends to apply the axial tensile load [5].

Table 1

Specimen Geometry

Specimen	lg-150	Lg-138	lg-100	lg-50
Gage length, l_g (mm)	150	138	100	50
Total Length, L (mm)	230	218	180	130
Width, w (mm)	15			
Thickness, t (mm)	0.22			
Fibre Density (g/cm^3)	1.79			
Nominal fiber volume (%)	57.42			

Note: The specimen designation is based on the gage length

Tensile test is carried out according to the guidelines from the standards ASTM D3039 [5], using 10kN Universal Testing Machine. The specimen is placed into the wedge grips of the mechanical testing machine and loaded in tension under loading rate 2mm/min. Loading continues to ultimate failure, where the tensile strength are determined. Load-displacement of the specimen is recorded throughout the test until fracture occurs.

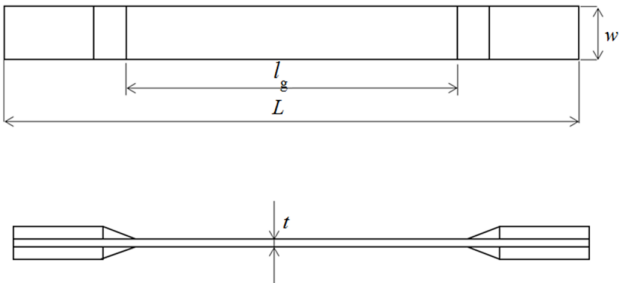

Fig. 1. Schematic diagram of specimen geometry

3. Finite Element Modeling

Finite element (FE) simulation using Abaqus is performed intended for the comparison with experimental test response during tensile loading. From the result, if the fibers in the lamina are perfectly aligned, there will be no different in tensile properties. Lamina is discretized using continuum shell elements (SC8R) while the tabs are idealized as mathematically rigid body with frictionless contact. For each specimens, the boundary conditions and loadings are imposed according to experimental test as illustrated in Fig. 2. The lamina is modeled as an equivalent orthotropic layer with elastic, damaging responses as described by Hashin's damage model [11]. The mechanical properties and the damage parameters of the CFRP lamina are listed in Table 2.

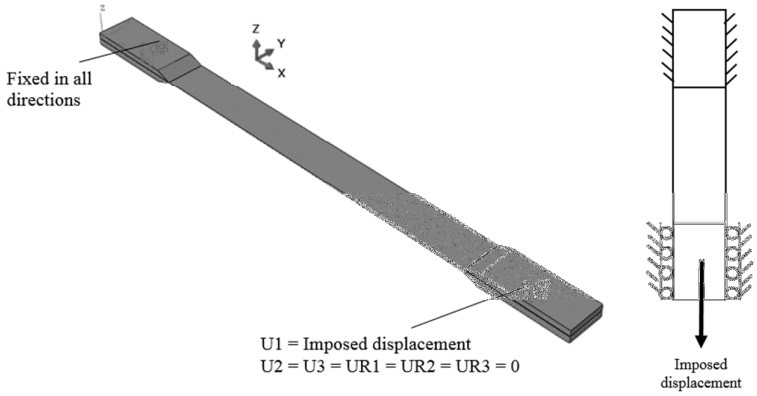

Fig. 2. FE Model of CFRP lamina under tensile test set up

Table 2
Elastic Properties and Model Parameters for Unidirectional Lamina of CFRP Composite [10]

Lamina constant		Magnitude	Lamina damage model parameters		Magnitude
Elastic modulus	E_{11}	105.5 GPa	Longitudinal tensile strength	X^T	1729 MPa
	E_{22}	7.2 GPa	Longitudinal compressive strength	X^C	1536.4 MPa
	E_{33}	7.2 GPa	Transverse tensile strength	Y^T	42.2 MPa
Shear modulus	G_{12}	3.4 GPa	Transverse compressive strength	Y^C	144 MPa
	G_{13}	3.4 GPa	Longitudinal shear strength	S^L	72.2 MPa
	G_{23}	2.52 GPa	Transverse shear strength	S^T	30 MPa
Poisson ratio	υ_{12}	0.34	Longitudinal tensile fracture energy	G_{XT}	62.4 N/mm
	υ_{13}	0.34	Longitudinal compressive fracture energy	G_{XC}	77.7 N/mm
	υ_{23}	0.378	Transverse tensile fracture energy	G_{YT}	9 N/mm
			Transverse compressive fracture energy	G_{YC}	13 /mm

4. Results and Discussion

a. Tensile response

The measured load-displacement responses of the composite specimen under tensile loading for 4 different gage length are shown in Figure 3. It was observed that multiple fiber fracture occurred, which are indicated by noticeable load drop before final fracture. This is the effect due to occurrence of fiber misalignment as shown in SEM image (Figure 4). The effect of this occurrences will be discussed in Section 4.2. From Figure 3 the slope of load-displacement curve is decreasing as the gage length of the specimen increase. This is due to averaging of unidirectionality of the fiber alignment in the lamina.

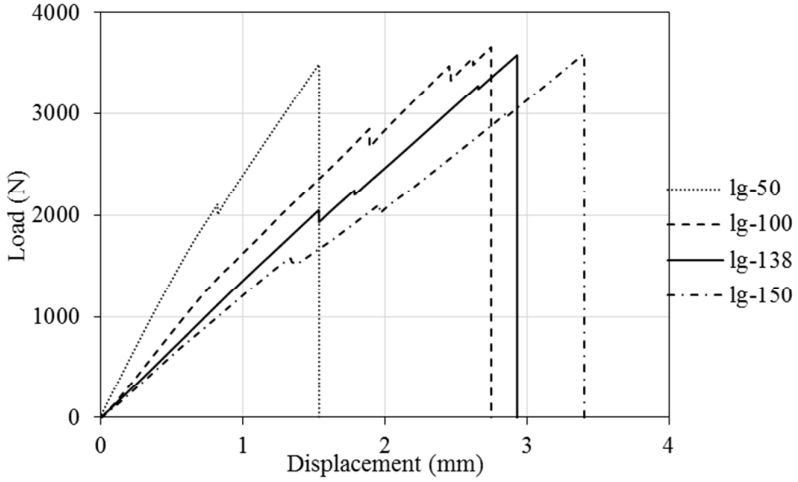

Fig. 3. Experimental load-displacement response of CFRP Lamina

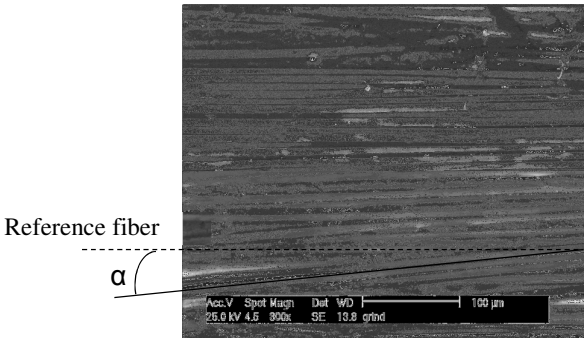

Fig. 4. Microscopy image of fiber alignment in a lamina

Table 3 compares the obtained tensile properties of different gage length from experiment. From Figure 5 when the specimen is pulled to the same displacement for every gage length, it can be seen that the elastic modulus is higher for the specimen with longer gage length. However the value of the modulus is levelling off from gage length 138mm to 150mm, where 138mm is the gage length suggested by ASTM. Figure 6 illustrates the significant effect of fiber misalignment as function of gage length.

Table 3
Tensile properties obtained form the experiment

Tensile Properties	Lg-150	Lg-138	Lg-100	Lg-50
Tensile Modulus of Elasticity (MPa)	55930	55930	42851	36960
Ultimate Tensile Stress (MPa)	1056	1085	1110	1106

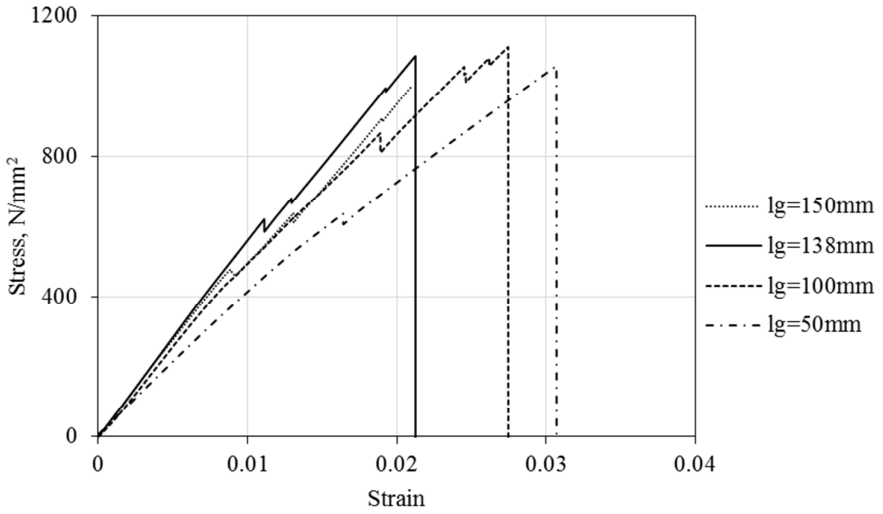

Fig. 5. Calculated stress-strain response of CFRP Lamina for various gage length

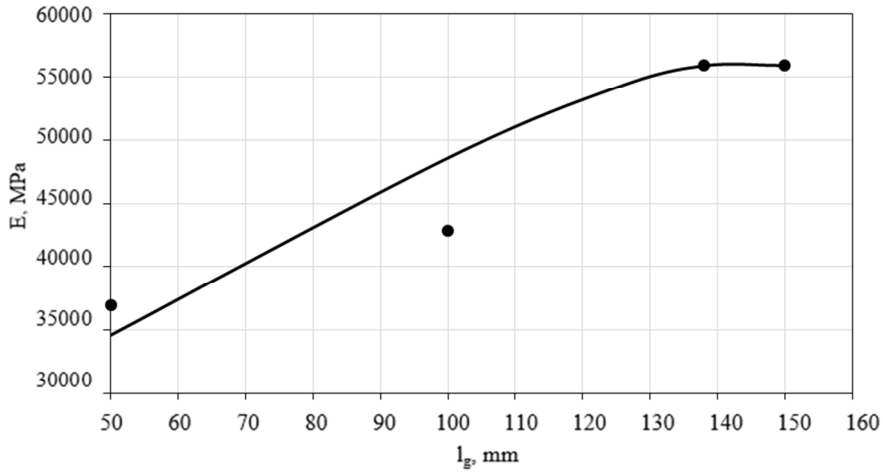

Fig. 6. Relation of gage length and modulus of elasticity

4.2 The Effect of Fiber Misalign to the Gage Length

The fiber alignment was calculated based on the SEM image. Briefly, the misalignment of the fiber is up to 7° from the reference fiber. From Figure 4, it can be calculated that the misaligned fiber is about 23.5% from total fiber count, where it is sufficient to affect the internal response in the lamina. The fiber misalignment is due to the fabrication process that affecting the load-displacement response which is resulted of those misaligned fiber will break earlier before reaching its tensile strength. A schematic diagram to explain this phenomena is shown in Fig. 7.

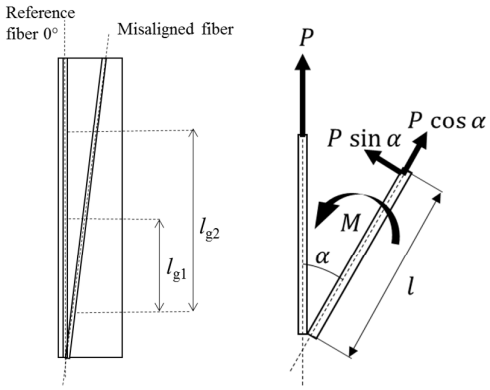

Fig. 7. Schematic diagram to explain the effect of the non-unidirectionality fiber alignment

The misalignment of the fiber will add additional stress to the total stress acting on the lamina during tensile loading (Equation (1)). As the gage length, l_g increase the bending stress, M is increasing, since the distance,l will increase (Equation (2)). As the result, stiffness reduction was encountered.

$$\sigma = \frac{P}{A} + \frac{My}{I} \tag{1}$$

where, P is applied load; A is cross sectional area of the specimen; M is the calculated bending moment given by Equation (2); y is the vertical distance away from the fiber neutral axis; I is the moment of inertia around the neutral axis of the fiber.

$$M = Psin\alpha \cdot l \tag{2}$$

where α is the angle given by the misaligned fiber from the reference 0°-fiber; while l is the moment arm.

4.3 Finite Element (FE) Simulation

FE Simulation and experimental results are compared for every gage length in terms of the load-displacement response. Fig. 8 indicated a fairly good comparison in the elastic region where no damage occurred yet. However after noticeable load drop in the experimental result there is deviation between experimental and FE curve. The deviation of experimental curve is due to the fiber breakage as described in Section 4.2 where it is not able to be captured thru FE simulation. From FE simulation result, Hashin Damage Model indicated that fiber and matrix damage in the lamina only occurred simultaneously during final fracture.

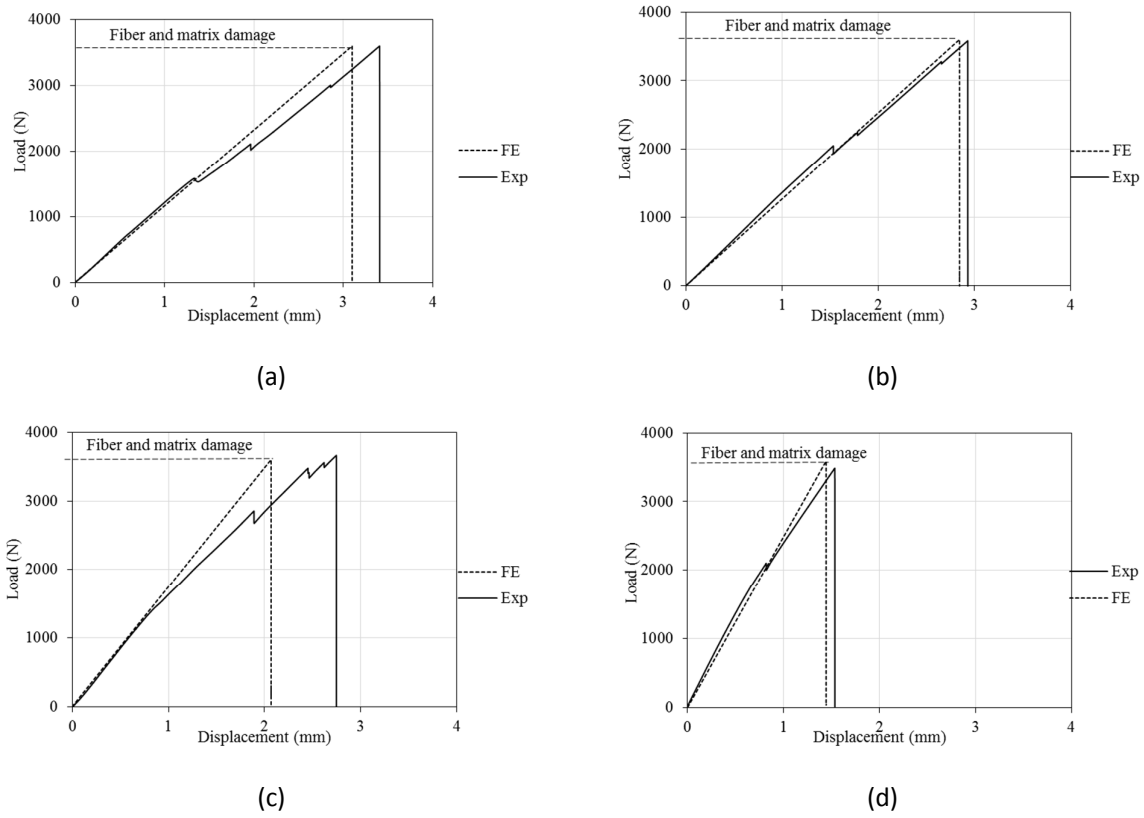

Fig. 8. Load-displacement response for (a)lg=150mm; (b)lg=138mm; (c)lg=100mm; (d)lg=50mm; from tensile experiment and FE simulation

5. Conclusion

The effect of fiber misalignment is not able to be captured thru FE simulation. However the gage length of the lamina during tensile test has made no significant difference in terms of parametric study where the effect of averaging is not been considered. Therefore for the computational time, the lamina can be simulated for different gage length (l_g<138mm) and will produce the reasonable response. Nevertheless, for damage analysis, experiment and FE only compared for l_g=138mm.

Acknowledgements

This work is funded by the Ministry of Higher Education Malaysia and Universiti Teknologi Malaysia through the Fundamental Research Grant Scheme (FRGS) No. 4F420

References

[1] Zhang, Xiao Yan, Yi Xiong, Xiao Jing Li, and Di Wang. "The development of virtual manufacturing technology." In *Applied Mechanics and Materials*, vol. 58, pp. 854-858. Trans Tech Publications, 2011.

[2] Umar, Zakaria, Abdul Azizz , Faieza, binti Hasan, Rosliza , Abdullah,Muhammad Babayo. "Virtual reality as industrial Training tool for manufacturing technology: A Review". *Journal of Advanced Review on Scientific Research* 31, no.1 (2017): 13-21

[3] Bowman, Doug A., Joseph L. Gabbard, and Deborah Hix. "A survey of usability evaluation in virtual environments: classification and comparison of methods." *Presence: Teleoperators & Virtual Environments* 11, no. 4 (2002): 404-424.

[4] Carpenter, I.D., Ritchie, J.M., Dewar, R.G., Simmons, J.E.L. "Virtual Manufacturing." *Manufacturing Engineers, IEEE*, UK, 76, (1997): 113-116.
[5] Usman, Mustapha M., Abdulrahaman S. Ahmad, Nuhu A. Sulaiman, and Musa A. Ibrahim. "Application of CAD/CAM Tools in the Production of Investment Casting Part."
[6] Ravi, B., and G. L. Datta. "Metal Casting–Back to Future." In *52nd Indian Foundry Congress*. 2004.
[7] Chwastyk, P., and M. Kolosowski. "Integration CAD/CAPP/CAM systems in design process of innovative products." In *Annals of DAAAM for 2012 & Proceedings of the 23rd International DAAAM Symposium, ISBN*, pp. 978-3. 2012.
[8] N. Rajaee, A. A. S. A Hussaini, A. Zulkharnain and S. M. W Masra. "Bio-inspired Computing for Network Modelling". *Journal of Advanced Research Design* 6, no1. (2015): 1-10
[9] Ravi, B. "Casting simulation and optimisation: benefits, bottlenecks and best practices." *Indian Foundry Journal* 54, no. 1 (2008): 47.
[10] Farin, Gerald E., Josef Hoschek, and Myung-Soo Kim, eds. *Handbook of computer aided geometric design*. Elsevier, 2002.
[11] Mattson, Mike. *CNC programming: principles and applications*. Cengage Learning, 2009.
[12] Farin, Gerald E. *Curves and surfaces for CAGD: a practical guide*. Morgan Kaufmann, 2002.
[13] Radhaakrishnan, P, Subramanyan S, Raju, V. CAD/CAM/CIM. New Delhi: New Age International (P) Limited, 2008.
[14] Kong, Jian and Song, Yanliang. "Analysis on the application of modern manufacturing-Oriented CAD/CAM". *Journal of Theoretical and Applied Information Technology* 50, no.3 (2013): 50.
[15] Narayan, Lalit K, Mallikarjuna Rao K, Sarcar MM. Computer Aided Design and Manufacturing. New Delhi: Prentice Hall of India Learning Private Limited, 2013.
[16] Kalpakjian, Serope, Steven R. Schmid, and Hamidon Musa. *Manufacturing engineering and technology: machining*. China Machine Press, 2011.
[17] Xu, Xun. "Integrating Advanced Computer-Aided Design, Manufacturing, and Numerical Control." *Information Science Reference* (2009).
[18] Ahmad, Suhairi Bin. "Application of PRO/Engineer in CAD/CAM". Assessed November 10, 2017. http://www.ptss.edu.my
[19] Ping, T. Y. Advanced Manufacturing Technology. P.R China: China Press, 2002.
[20] Pratt, Michael J. "Virtual prototypes and product models in mechanical engineering." In *Virtual Prototyping*, pp. 113-128. Springer, Boston, MA, 1995.